Cancer Immunol Immunother (2016) 65:1365–1375
DOI 10.1007/s00262-016-1894-6

ORIGINAL ARTICLE

The role of Ly49E receptor expression on murine intraepithelial lymphocytes in intestinal cancer development and progression

Aline Van Acker[1] · Els Louagie[2] · Jessica Filtjens[1] · Sylvie Taveirne[1] · Els Van Ammel[1] · Tessa Kerre[1] · Dirk Elewaut[2] · Tom Taghon[1] · Bart Vandekerckhove[1] · Jean Plum[1] · Georges Leclercq[1]

Received: 17 February 2016 / Accepted: 26 August 2016 / Published online: 1 September 2016

Abstract Ly49E is a member of the Ly49 family of NK receptors and is distinct from other members of this family on the basis of its structural properties, expression pattern and ligand recognition. Importantly, Ly49E receptor expression is high on small intestinal and colonic intraepithelial lymphocytes (IELs). Intestinal IELs are regulators of the mucosal immune system and contribute to front-line defense at the mucosal barrier, including anti-tumor immune response. Whereas most Ly49 receptors have MHC class-I ligands, we showed that Ly49E is instead triggered by urokinase plasminogen activator (uPA). uPA has been extensively implicated in tumor development, where increased uPA expression correlates with poor prognosis. As such, we investigated the role of Ly49E receptor expression on intestinal IELs in the anti-tumor immune response. For this purpose, we compared Ly49E wild-type mice to Ly49E knockout mice in two established tumor models: $Apc^{Min/+}$-mediated and azoxymethane-induced intestinal cancer. Our results indicate that Ly49E expression on IELs does not influence the development or progression of intestinal cancer.

Keywords Ly49E · Urokinase plasminogen activator · Intraepithelial lymphocyte · Intestinal cancer

Abbreviations

AOM	Azoxymethane
DSS	Dextran sodium sulfate
IEL	Intestinal intraepithelial lymphocyte
KO	Knockout
uPA	Urokinase plasminogen activator
WT	Wild-type

Introduction

Colorectal cancer represents the third most common type of cancer worldwide [1, 2]. Of all cases, 10–30 % are hereditary, such as familial adenomatous polyposis coli and hereditary non-polyposis colon cancer. The majority, however, can be attributed to non-familial sporadic mutations and colitis-associated cancer [3]. For patients, treatment options today are limited. Curative resection in combination with chemo- or radiotherapy is standard, but recurrence rates are high, and up to 50 % [4]. Alongside, a variety of new immunotherapies have been developed, including peptide-, whole tumor lysate-, dendritic cell- and viral vector-based vaccines. Adoptive cell transfer, including chimeric antigen receptor therapy, and antibody-based therapies have also been introduced [5]. However, all currently available therapies struggle with low efficiency and limited success rates [5]. Therefore, sustained and additional research to elucidate the mechanisms that operate in intestinal cancer progression and development are crucial to improve outcome in therapies.

IELs are key to maintaining intestinal homeostasis. Strategically positioned within the intestinal epithelium, these

Electronic supplementary material The online version of this article (doi:10.1007/s00262-016-1894-6) contains supplementary material, which is available to authorized users.

✉ Georges Leclercq
georges.leclercq@ugent.be

[1] Department of Clinical Chemistry, Microbiology and Immunology, Ghent University, De Pintelaan 185, 9000 Ghent, Belgium

[2] Department of Rheumatology, Unit for Molecular Immunology and Inflammation, VIB Inflammation Research Center, Ghent University, Ghent, Belgium

cells have been implicated in the recognition of stress signals [6] and repair of the intestinal epithelium [7]. Furthermore, IELs have been attributed a role in intestinal tumor immune response as demonstrated by a number of in vitro and in vivo studies. Cytotoxicity of intestinal IELs toward epithelial cell tumors was first reported in 1993 [8]. Later, Ebert et al. [9] showed that interaction of CD2 on the IEL surface with tumor-expressed CD58 induces expression of IL-8, TNF-α and IFN-γ by IELs, with a resulting enhanced anti-tumor response. Additionally, binding of IEL-expressed NKG2D to tumor MIC and ULBP ligands may trigger Fas-mediated lysis of tumor cells [10]. Moreover, Baker et al. [11] showed that colorectal cancers preferentially retain intestinal IEL rather than peripherally derived CD8 T cells. Together, these data illustrate that IELs, and NK receptors expressed on the IEL cell surface, play an important role in mediating intestinal tumor immune response.

Ly49E is an inhibitory member of the Ly49 NK receptor family [12], characterized by a unique expression profile. Ly49E expression is high on tissue-resident lymphocytes, including CD8αα-positive IEL [13, 14]. IELs expressing inhibitory Ly49 receptors, including Ly49E, are hyporesponsive to TCR-mediated stimulation [13]. Importantly, in vitro TCR-triggering results in upregulation of Ly49E receptor expression on IELs [15]. Furthermore, whereas all other inhibitory Ly49 receptors have MHC class-I ligands, Ly49E is triggered by the non-MHC-related protein uPA [16]. Importantly, uPA has been implicated in tumor development in general, and colorectal cancer in particular, as an increase in tumor uPA expression has been noted in the colorectal adenoma-carcinoma transition [17–22]. Also, in a clinical setting, increased uPA levels have been linked to poor patient prognosis [23, 24]. Indeed, targeted uPA antibodies and inhibitors have been shown to reduce tumor growth, cancer cell spread and metastasis [25, 26].

With the recent finding that uPA triggers the inhibitory Ly49E receptor, along with the observed constitutive expression of Ly49E on intestinal IELs and its additional upregulation upon TCR-mediated activation, we hypothesize that Ly49E receptor expression by IELs affects their in vivo immune response toward intestinal tumors. If this hypothesis is correct, uPA produced by tumor cells would not only promote tumor invasion and metastasis, but would also be used as a novel tumor escape mechanism from host innate-like T cells. We tested this hypothesis by comparing Ly49E KO to Ly49E WT mice in two intestinal tumor models, $Apc^{Min/+}$-mediated and azoxymethane (AOM)-induced colorectal cancer. $Apc^{Min/+}$ mice were first described in 1990, and have been used extensively since for the study of intestinal tumor development [27]. In humans, 80 % of sporadic colorectal cancers have a mutation in the *Apc* gene [28]. Moreover, mutations in *Apc* are present in familial adenomatous polyposis coli [28]. Alongside, the AOM-induced colorectal cancer model accurately recapitulates the aberrant crypt foci-adenoma-carcinoma sequence and allows for the development of adenocarcinomas in a relatively short time span [29, 30]. Furthermore, tumors develop almost exclusively in the middle to distal colon, mimicking human colorectal cancer [29]. Using these two intestinal tumor mouse models, we show that tumor-infiltrating IEL are predominantly CD4 and CD8αβ TCRαβ cells. Importantly, IEL Ly49E receptor expression by IELs did not influence the development or progression of intestinal cancer.

Materials and methods

Mice

Ly49E KO mice were generated as previously described [31]. Heterozygous $Apc^{Min/+}$ mice were purchased from Jackson Laboratories (Bar Harbor, ME, USA). Male $Apc^{Min/+}$ $Ly49E^{WT/WT}$ mice were first bred to female $Apc^{+/+}$ $Ly49E^{KO/KO}$ mice, after which male heterozygous $Apc^{Min/+}$ $Ly49E^{WT/KO}$ offspring were bred to female heterozygous $Apc^{+/+}$ $Ly49E^{WT/KO}$ offspring to generate $Apc^{Min/+}$ $Ly49E^{WT/WT}$, $Apc^{Min/+}$ $Ly49E^{KO/KO}$, $Apc^{+/+}$ $Ly49E^{WT/WT}$ and $Apc^{+/+}$ $Ly49E^{KO/KO}$ mice. Mice were housed and bred in our animal facility, and all animal experimentation was approved and performed according to the guidelines of the Ethical Committee for Experimental Animals at the Faculty of Medicine and Health Sciences of Ghent University (Ghent, Belgium).

Genotyping of mice

Tail genomic DNA was isolated using the REDExtract-N-Amp Tissue PCR Kit (Sigma-Aldrich, St. Louis, MO, USA). PCR primers: *Apc* forward-5′-TGAGAAAGACAG AAGTTA-3′ and reverse-5′-TCCACTTTGGCATAAGGC-3′; *Ly49E* WT forward-5′-TCGCTTGGAATCTTCTGTTTC-3′ and reverse-5′TCCTCACCTGGACTGCAATC-3′; *Ly49E* KO forward-5′GGAATAATTGCTGTTACCATTAG and reverse-5′TCCTCACCTGGACTGCAATC-3′. The Apc^{Min} allele yields a PCR fragment of 313 bp, whereas the Apc WT allele does not yield a PCR fragment due to primer mismatch. Ly49E WT and KO alleles yield PCR fragments of 1070 and 1200 bp, respectively.

AOM-induced colorectal cancer

AOM-induced colorectal cancer was induced in 7–11-week-old mice. At day 0, mice were intraperitoneally injected with 10 mg/kg AOM (Sigma-Aldrich, St. Louis, MO, USA). At day 7, 2.5 % (v/w) dextran sodium sulfate

(DSS) (molecular weight 36,000–50,000, MP Biomedicals, Cleveland, OH, USA) was administered in drinking water and mice were allowed to drink ad libitum for 7 days. Thereafter, drinking water containing DSS was replaced by normal drinking water and mice were allowed to recover. At days 28 and 39, a second and third DSS-treatment cycle (2 % DSS in drinking water) was initiated. Control mice were not treated with AOM, but were subjected to DSS treatment in an identical manner to AOM-treated mice.

Assessment of mouse weight, intestinal length and tumor load/distribution

Mice were weighed weekly, and at each time point of analysis. After killing by cervical dislocation, the small intestine or colon was removed and intestinal length was determined. Intestines were cleaned of all mesentery and cut open longitudinally for microscopic analysis of tumor load, size and distribution. The maximal tumor diameter was used to determine tumor size. For tumor distribution, intestines were cut into three equal-sized segments and the number of tumors per segment was noted.

Isolation of tumor-infiltrating intestinal IELs

Tumor-rich sections of the small intestine, or dissected colonic and colorectal tumors, were obtained. Subsequently, infiltrating IELs were isolated as previously described [14].

Antibodies

mAbs used for staining were as follows: anti-TCRβ (APC/Cy7-conjugated, clone H57.597), anti-CD4 (peridinin chlorophyll protein/Cy5.5-conjugated, clone GK1.5), anti-CD8β (peridinin chlorophyll protein/Cy5.5-conjugated, clone YTS156.7.7), all from BioLegend (San Diego, CA, USA). Anti-TCRδ (PE- or FITC-conjugated, clone GL3), obtained from Becton–Dickinson, (Franklin Lakes, NJ, USA). Anti-CD8α (PE/Cy7-conjugated, clone 53-6.7) from eBioscience (San Diego, CA, USA). Anti-Ly49C/E (biotin-conjugated, clone 4D12, made and labeled in-house) [32] and anti-Ly49E/F (FITC-conjugated, clone CM4; kindly provided by Dr C. G. Brooks (Newcastle on Tyne, UK)) [33]. mAb 4D12 (Ly49C/E) in combination with mAb CM4 (Ly49E/F) were used to identify Ly49E-expressing cells ($CM4^+/4D12^+$), Ly49C-expressing cells ($CM4^-/4D12^+$) and Ly49F-expressing cells ($CM4^+/4D12^-$). Cells were blocked with anti-FcγRII/III (unconjugated, clone 2.4G2, kindly provided by Dr J. Unkeless, Mount Sinai School of Medicine, New York, NY, USA), and propidium iodide was used to discriminate live and dead cells. Flow cytometric analysis was performed using a BD LSRII flow cytometer, and samples were analyzed with FACSDiva Version 6.1.2 software (BD Biosciences).

Immunohistochemistry

Tumor-rich sections of the distal ileum and distal colon were fixed in 4 % formaldehyde solution (VWR, Radnor, PA, USA) and embedded in paraffin. Five milliliters formalin-fixed paraffin-embedded sections was stained with hematoxylin and eosin (Sigma-Aldrich) for analysis of tumor morphology. Alternately, sections were immersed in target retrieval solution, pH6 (Dako, Glostrup, Denmark) for 20 min at 95 °C for antigen retrieval. Subsequently, sections were stained for immunofluorescent analysis of tumor-infiltrating lymphocytes. Antibodies used for immunofluorescent staining were polyclonal rabbit anti-human/mouse CD3 (Dako) and Dylight649 donkey anti-rabbit (BioLegend). Cell nuclei were counterstained by mounting with ProLong Gold antifade reagent with DAPI (Invitrogen). Stained sections were analyzed on a Leica TCS SPE (Leica Microsystems, Wetzlar, Germany) using the LAS4, LASAF and ImageJ software.

uPA ELISA

Tumors were microscopically dissected and weighed. Subsequently, tumors were lysed in buffer composed of 1 part PBS/1 part caspase lysis buffer/2 parts blocking buffer (0.1 M Tris, 0.15 M NaCl, 3 % BSA, pH 7.4), on a Precellys24 tissue homogenizer (Bertin Technologies, Montigny-le-Bretonneux, France). The uPA content of the tumor lysates was determined using the Mouse uPA Total ELISA Kit (Innovative Research, Novi, MI, USA). Results are expressed as ng uPA per mg of tumor tissue.

Statistics

Statistical analysis was carried out using PASW Statistics 22 Software (SPSS, Chicago, IL, USA). Data were analyzed using the nonparametric two-tailed Mann–Whitney *U*-test, or the Kruskall–Wallis test. A p value ≤ 0.05, (*), a p value ≤ 0.01 (**) and p value ≤ 0.001 (***), were considered statistically significant.

Results

Mouse weight, small intestinal length and tumor load are unaltered in $Apc^{Min/+}$ mice on an Ly49E KO background

To study the role of Ly49E in intestinal cancer development and progression in $Apc^{Min/+}$ mice, we generated $Apc^{Min/+}$ Ly49E WT and $Apc^{Min/+}$ Ly49E KO littermates. Mice were

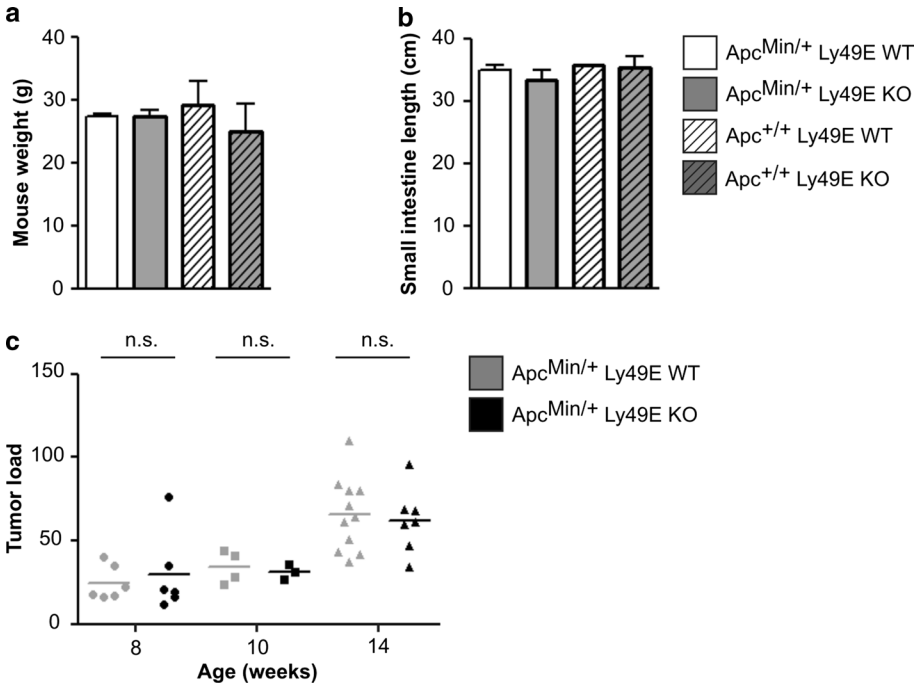

Fig. 1 Apc-mediated intestinal cancer on a Ly49E KO background. **a** Body weight of Apc$^{Min/+}$ Ly49E WT and Apc$^{Min/+}$ Ly49E KO mice (mean ± SEM; $n = 10$ for Apc$^{Min/+}$ Ly49E WT, $n = 5$ for Apc$^{Min/+}$ Ly49E KO) and control Ly49E WT and Ly49E KO littermates (mean ± SEM; $n = 6$) at 14 weeks of age. **b** Length of the small intestine in Apc$^{Min/+}$ Ly49E WT and Apc$^{Min/+}$ Ly49E KO mice (mean ± SEM; $n = 5$ for Apc$^{Min/+}$ Ly49E WT, $n = 3$ for Apc$^{Min/+}$ Ly49E KO) and Ly49E WT and Ly49E KO littermates (mean ± SEM; $n = 3$) at 14 weeks of age. **c** Tumor load in the small intestine of Apc$^{Min/+}$ Ly49E WT and Apc$^{Min/+}$ Ly49E KO mice at 8, 10 and 14 weeks of age

weighed at 14 weeks of age, when tumor load was highest. Mouse weight did not differ significantly between Apc$^{Min/+}$ Ly49E WT and Apc$^{Min/+}$ Ly49E KO littermates, nor between Apc$^{Min/+}$ and control Apc$^{+/+}$ littermates (Fig. 1a). To investigate whether *Ly49e* gene expression influences intestinal length in Apc^{Min} mice, we analyzed small intestinal length in Apc$^{Min/+}$ Ly49E WT and Apc$^{Min/+}$ Ly49E KO littermates at 14 weeks of age. As illustrated in Fig. 1b, small intestinal length was unchanged between Apc$^{Min/+}$ Ly49E WT and Apc$^{Min/+}$ Ly49E KO littermates, and between Apc$^{Min/+}$ and control Apc$^{+/+}$ mice. When analyzing small intestine tumor size, we did not find tumor size to be different in Apc$^{Min/+}$ Ly49E WT as compared with Apc$^{Min/+}$ Ly49E KO mice, and all tumors that developed had a 1–2 mm diameter in size. When analyzing small intestine tumor load during aging, there was a clear increase in tumor load as mice aged from 8 to 14 weeks of age. However, tumor numbers were comparable between Apc$^{Min/+}$ Ly49E WT and Apc$^{Min/+}$ Ly49E KO littermates at all timepoints analyzed (Fig. 1c). Tumor distribution, i.e., in the proximal, middle or distal parts of the small intestine, was also similar for Apc$^{Min/+}$ Ly49E WT and Apc$^{Min/+}$ Ly49E KO littermates (data not shown). As expected, no intestinal tumors were detected in Apc$^{+/+}$ mice (data not shown).

Tumor-infiltrating T cells and tumor uPA expression levels are similar between Apc$^{Min/+}$ Ly49E WT and Apc$^{Min/+}$ Ly49E KO mice

To examine possible differences in tumor-infiltrating T lymphocytes in Apc$^{Min/+}$ Ly49E WT and Apc$^{Min/+}$ Ly49E KO littermates, we first stained tumor sections for CD3$^+$ T cells. As illustrated in Fig. 2a, tumor-infiltrating T cells were clearly present, with tumor size inversely correlated to the number of infiltrating T cells/mm^2. However, we did not observe discernible differences in the numbers of tumor-infiltrating T cells between Apc$^{Min/+}$ Ly49E WT and Apc$^{Min/+}$ Ly49E KO mice. To investigate possible changes in subpopulations of tumor-infiltrating T lymphocytes between Apc$^{Min/+}$ Ly49E WT and Apc$^{Min/+}$ Ly49E KO littermates, tumor-infiltrating IEL were isolated from tumor-rich tissue and population frequencies were analyzed, and compared to IEL subpopulations of Apc$^{+/+}$ littermate mice. At 14 weeks of age, we noted a slight increase in TCRαβ lymphocytes, and decrease in TCRγδ lymphocytes, for Apc$^{Min/+}$ mice compared to Apc$^{+/+}$ mice. TCRαβ and TCRγδ lymphocyte frequencies were not different in tumor-infiltrating T lymphocytes of Apc$^{Min/+}$ mice on an Ly49E WT versus Ly49E KO background. Within the TCRαβ lymphocyte fraction, we observed no differences between CD4, CD8αβ and CD8αα subpopulations. Within the TCRγδ lymphocyte fraction, CD4/CD8 double-negative and CD8αα cell frequencies were unchanged (Fig. 2b). Ly49E is expressed almost exclusively by CD8αα-expressing IEL [14]. The frequency of Ly49E-expressing TCRαβ CD8αα and TCRγδ CD8αα IELs did not differ significantly between Apc$^{Min/+}$ Ly49E WT and Apc$^{+/+}$ Ly49E WT littermates (data not shown), and IELs from Apc$^{Min/+}$ Ly49E KO mice did not express Ly49E (supplementary Fig. 1). We have previously shown that uPA triggers Ly49E and that this results in inhibition of cytotoxicity as well as cytokine production of Ly49E-expressing lymphocytes

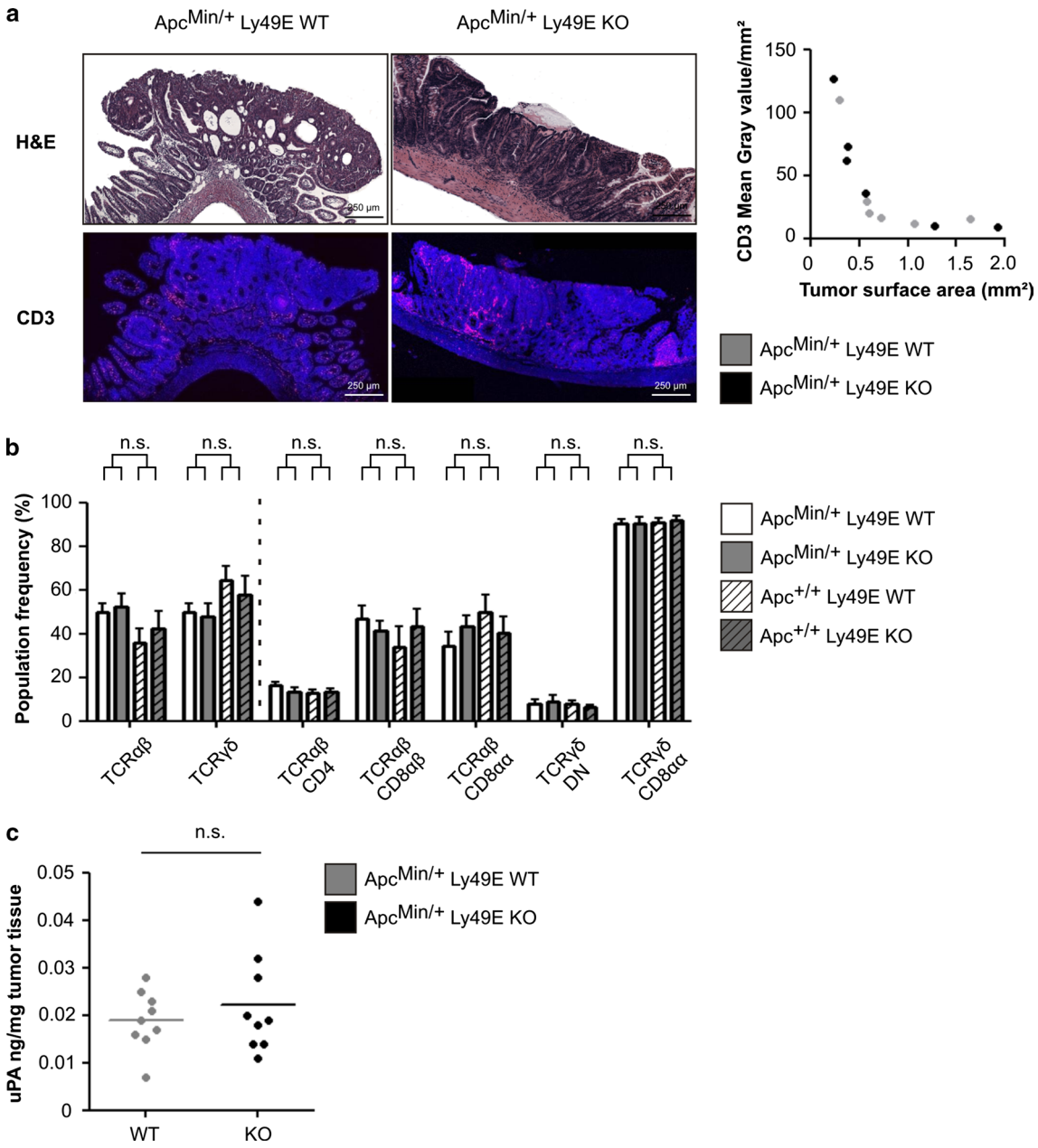

Fig. 2 Tumor-infiltrating T cells and tumor uPA expression in Apc$^{Min/+}$ Ly49E WT versus Apc$^{Min/+}$ Ly49E KO mice. **a** Hematoxylin/eosin- (*upper*), and CD3-(*lower*) stained paraffin tumor sections from Apc$^{Min/+}$ Ly49E WT and Apc$^{Min/+}$ Ly49E KO mice. Scale bar: 250 µm, ×100 magnification. A graph showing CD3 mean gray value/mm^2 according to tumor surface area (mm^2) is shown for Apc$^{Min/+}$ Ly49E WT and Apc$^{Min/+}$ Ly49E KO mice ($n = 6$). **b** Small intestinal tumor-infiltrating IEL subpopulation frequencies in Apc$^{Min/+}$ Ly49E WT and Apc$^{Min/+}$ Ly49E KO mice, and small intestinal IEL subpopulation frequencies from control littermates, at 14 weeks of age (mean ± SEM; $n = 6$). The percentage of TCRαβ and TCRγδ IEL is shown as a fraction of the total numbers of T cells. TCRαβ CD4, TCRαβ CD8αβ and TCRαβ CD8αα IEL subpopulation frequencies are shown as a percentage of the total TCRαβ IELs. TCRγδ DN and TCRγδ CD8αα IEL subpopulation frequencies are shown as a percentage of total TCRγδ IEL. **c** Tumor uPA expression in tumors from Apc$^{Min/+}$ Ly49E WT and Apc$^{Min/+}$ Ly49E KO mice at 14 weeks of age. *n.s.* not significant

[16]. Furthermore, extensive research has shown that uPA is critical in tumor development and metastasis [24, 25, 34]. To investigate a putative link between Ly49E and tumor uPA expression levels, we analyzed uPA expression levels in lysates of intestinal tumors from Apc$^{Min/+}$ Ly49E WT versus Apc$^{Min/+}$ Ly49E KO mice. In parallel, uPA expression in healthy control, non-tumor intestinal tissue from Ly49E WT and Ly49E KO mice was determined. uPA expression levels in healthy control tissue were low, and not significantly different for Ly49E WT (0.0010 ± 0.0001 ng/

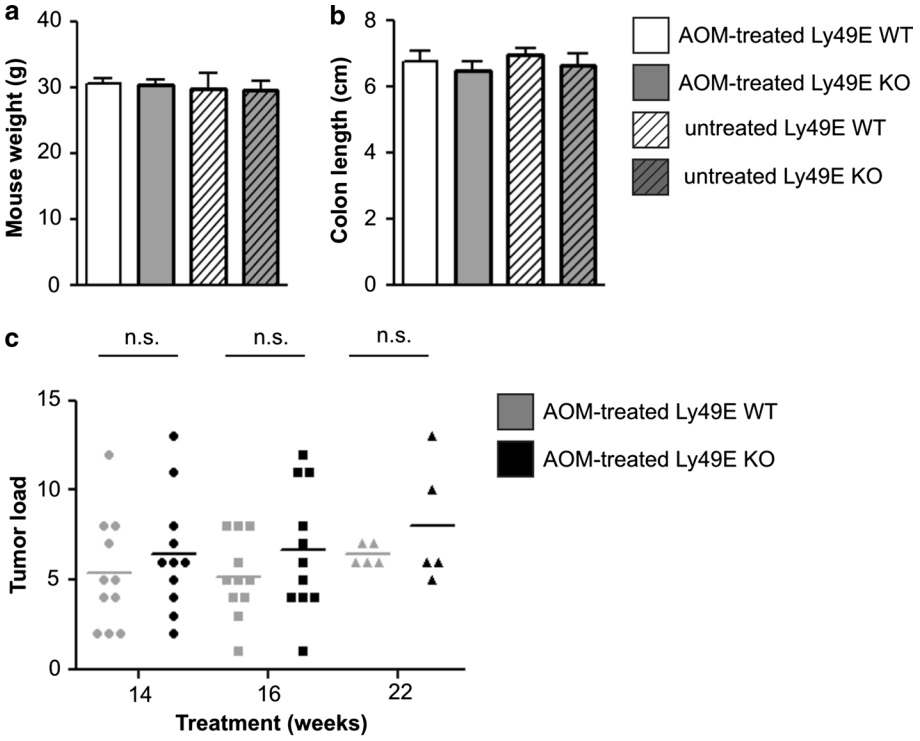

d

	Treatment (weeks)	Average number of tumors		
		≤ 2 mm	3-4 mm	≥ 5 mm
Ly49E WT	14	1.00 ± 1.00	2.33 ± 1.15	0.67 ± 0.58
Ly49E KO		4.67 ± 2.31	0.67 ± 1.15	0.33 ± 0.58
Ly49E WT	16	2.83 ± 1.72	1.50 ± 1.38	0.83 ± 0.75
Ly49E KO		4.00 ± 0.63	0.50 ± 0.84	1.17 ± 1.60
Ly49E WT	22	4.80 ± 1.79	1.20 ± 1.64	0.40 ± 0.55
Ly49E KO		4.80 ± 2.28	1.60 ± 1.14	1.60 ± 0.89

Fig. 3 AOM-induced colorectal cancer on a Ly49E KO background. **a** Body weight of AOM-treated Ly49E WT and Ly49E KO mice (mean ± SEM; $n = 8$ for AOM-treated Ly49E WT, $n = 7$ for AOM-treated Ly49E KO) 22 weeks following the start of treatment, and of untreated mice at a similar age (mean ± SEM; $n = 5$). **b** Colon length of AOM-treated Ly49E WT and Ly49E KO mice (mean ± SEM; $n = 8$ for AOM-treated Ly49E WT, $n = 7$ for AOM-treated Ly49E KO) 22 weeks following the start of treatment, and of untreated mice at a similar age (mean ± SEM; $n = 4$). **c** Colon tumor load in AOM-treated Ly49E WT and Ly49E KO mice at 14, 16 and 22 weeks following the start of treatment. **d** Average number of tumors, when tumors are classified according to size, in AOM-treated Ly49E WT and Ly49E KO mice at 14, 16 and 22 weeks following the start of treatment (mean ± SEM; $n = 3$ at 14 weeks, $n = 6$ at 16 weeks and $n = 5$ at 22 weeks). *n.s.* not significant

mg intestinal tissue) as compared to Ly49E KO mice (0.0008 ± 0.0003 ng/mg intestinal tissue). Tumor uPA expression exceeded expression of uPA in healthy tissue at least 10 times. However, tumor uPA expression levels were comparable between $Apc^{Min/+}$ Ly49E WT and $Apc^{Min/+}$ Ly49E KO mice (Fig. 2c).

Mouse weight, colon length and colon tumor load are similar between AOM-treated Ly49E WT and Ly49E KO mice

To induce tumor formation in the colon, Ly49E WT and Ly49E KO mice were administered 10 mg/kg AOM and subsequently subjected to 3 cycles of DSS treatment, eliciting colitis-associated colorectal cancer. Mice were analyzed at 14, 16 and 22 weeks following the start of treatment. At 22 weeks, mouse weight was unchanged between AOM-treated and untreated control mice. Moreover, we did not observe weight differences between AOM-treated Ly49E WT and AOM-treated Ly49E KO mice (Fig. 3a). As severe colitis is linked to colon shortening [1], we analyzed colon length in untreated and AOM-treated mice. Colon length was not significantly altered in AOM-treated Ly49E KO as compared to AOM-treated Ly49E WT mice, nor in AOM-treated versus untreated mice (Fig. 3b). When analyzing colon tumor load, we observed that tumors of varying size developed and that tumor load increased as treatment progressed. In tumors ≤2 mm, we observed a slightly greater tumor load for Ly49E KO as compared to AOM-treated Ly49E WT mice. In contrast, in tumors ≥5 mm, tumor load for AOM-treated Ly49E WT mice was greater than that of AOM-treated Ly49E KO mice. However, these differences were not significant ($p = 0.281$ for ≤2 mm tumors, $p = 0.689$ for ≥5 mm tumors) and overall tumor load was comparable between AOM-treated Ly49E KO and AOM-treated Ly49E WT mice (Fig. 3c). We did not note significant differences in tumor size (Fig. 3d). Alongside, tumor distribution was similar for AOM-treated

Ly49E WT as compared to Ly49E KO mice, with tumor development almost exclusively restricted to the middle and distal colon (data not shown), as has been reported previously [29].

Tumor-infiltrating T cell frequencies and tumor uPA expression levels are unchanged in AOM-treated Ly49E WT versus Ly49E KO mice

As illustrated in Fig. 4a, immunofluorescent staining for tumor-infiltrating T cells shows that small tumors have relatively more infiltrating T cells/mm^2 than large tumors. However, there were no discernible differences in the frequencies of tumor CD3$^+$ infiltrating cells between AOM-treated Ly49E WT and AOM-treated Ly49E KO mice. Following dissection of colorectal tumors, the frequencies of tumor-infiltrating T lymphocyte subsets were analyzed. We observed a strong and statistically significant increase in the frequency of TCRαβ ($p = 0.013$) and a decrease in TCRγδ ($p = 0.013$) tumor-infiltrating lymphocytes, as compared to IELs from untreated mice. Within the TCRαβ lymphocyte fraction of tumor-infiltrating lymphocytes, there was an increase in conventional CD4 lymphocytes ($p = 0.014$), and a corresponding decrease in the frequency of non-conventional CD8αα lymphocytes ($p = 0.012$). Surprisingly also, within the TCRγδ lymphocyte fraction, we noted a sharp increase in the frequency of DN lymphocytes ($p = 0.011$) and a corresponding decrease in CD8αα lymphocytes ($p = 0.011$) (Fig. 4b, c). However, we did not detect differences in lymphocyte population frequencies in AOM-treated Ly49E WT versus AOM-treated Ly49E KO mice. Moreover, the frequency of Ly49E-expressing TCRαβ CD8αα and TCRγδ CD8αα IELs did not differ significantly between AOM-treated Ly49E WT and untreated mice (data not shown), and IELs from AOM-treated Ly49E KO mice did not express Ly49E (supplementary Fig. 2). Lastly, we analyzed uPA expression by tumors of varying size, isolated from AOM-treated mice (Fig. 4d). Tumor uPA expression increased steadily as tumors grew larger in size (≤2 mm tumors: WT 0.009 ± 0.016, KO 0.014 ± 0.012; 3–4 mm tumors: WT 0.022 ± 0.023, KO 0.016 ± 0.014; ≥5 mm tumors: WT 0.043 ± 0.028, KO 0.030 ± 0.010; all ng/mg tumor tissue). In 3–4 mm and ≥5 mm tumors, there was a trend toward higher uPA expression in AOM-treated Ly49E WT versus Ly49E KO mice, possibly indicating a weak influence of the uPA-Ly49E interaction in selecting for tumors with higher uPA expression. However, the difference between AOM-treated Ly49E WT versus AOM-treated Ly49E KO mice was not significant ($p = 0.805$ for 3–4 mm tumors; $p = 0.689$ for ≥5 mm tumors).

Discussion

Apc$^{Min/+}$ mice are frequently used in the study of intestinal cancer development [27]. Here, we studied a possible role for Ly49E in cancer development using Apc$^{Min/+}$ mice crossed onto an Ly49E KO background. To investigate if Ly49E affects mouse weight, we weighed Apc$^{Min/+}$ Ly49E WT and Apc$^{Min/+}$ Ly49E KO mice at 14 weeks of age, when tumor load reached a plateau, as similarly observed by Puppa et al. [35]. Our results show no differences in body weight, suggesting that Apc$^{Min/+}$ -mediated pathology in these mice is similar. This was confirmed by the absence of a difference in small intestinal length between Apc$^{Min/+}$ Ly49E WT and Apc$^{Min/+}$ Ly49E KO littermates. Apc$^{Min/+}$ Ly49E WT and Apc$^{Min/+}$ Ly49E KO mice developed numerous 1–2 mm adenomatous polyps along the duodenal to ileal axis, with a 100 % penetrance. As has been previously reported, and in contrast to human colorectal cancers [27, 36], tumors developed almost exclusively in the small intestine and were not detected in the colon. Tumor load increased with age and was not significantly different in Apc$^{Min/+}$ Ly49E WT as compared to Apc$^{Min/+}$ Ly49E KO mice, indicating that adenoma formation and growth is not affected by Ly49E expression.

Immunofluorescent staining showed that global T cell infiltration is comparable between Apc$^{Min/+}$ Ly49E WT and Apc$^{Min/+}$ Ly49E KO mice. Marsh et al. [37] have previously shown that both Apc$^{Min/+}$ TCRβ$^{-/-}$ and Apc$^{Min/+}$ TCRδ$^{-/-}$ mice develop less tumors than Apc$^{Min/+}$ mice, implicating a role for both TCRαβ and TCRγδ cells in tumorigenesis. Examining tumor lymphocyte infiltration in Apc$^{Min/+}$ Ly49E WT and Apc$^{Min/+}$ Ly49E KO littermates and comparing these to IELs of Apc$^{+/+}$ littermate controls, we observed a slight increase in the frequency of TCRαβ cells, and decreased frequencies of TCRγδ cells. The latter is in agreement with Marsh et al. [37] who similarly recovered fewer TCRγδ cells from Apc$^{Min/+}$ as compared to Apc$^{+/+}$ mice. Frequencies of the CD4, CD8αα and/or CD8αβ subpopulations of TCRαβ and TCRγδ cells were unaltered between Apc$^{Min/+}$ and Apc$^{+/+}$ mice. Moreover, we observed no differences in infiltrating lymphocyte composition between Apc$^{Min/+}$ Ly49E WT and Apc$^{Min/+}$ Ly49E KO mice. Taken together, our data illustrate that Ly49E does not influence the number or frequencies of tumor-infiltrating lymphocytes in Apc$^{Min/+}$ mice.

Ploplis et al. [38] showed that Apc$^{Min/+}$ *Plau*$^{-/-}$ mice, which have an additional uPA deficiency, have a lower tumor load than Apc$^{Min/+}$ (*Plau*$^{+/+}$) mice. Our laboratory showed that uPA triggers the Ly49E receptor, thereby inhibiting cytokine production and cytotoxicity [16]. Furthermore, Ly49E expression on intestinal intraepithelial cells is high [13], where Ly49E is primarily expressed by

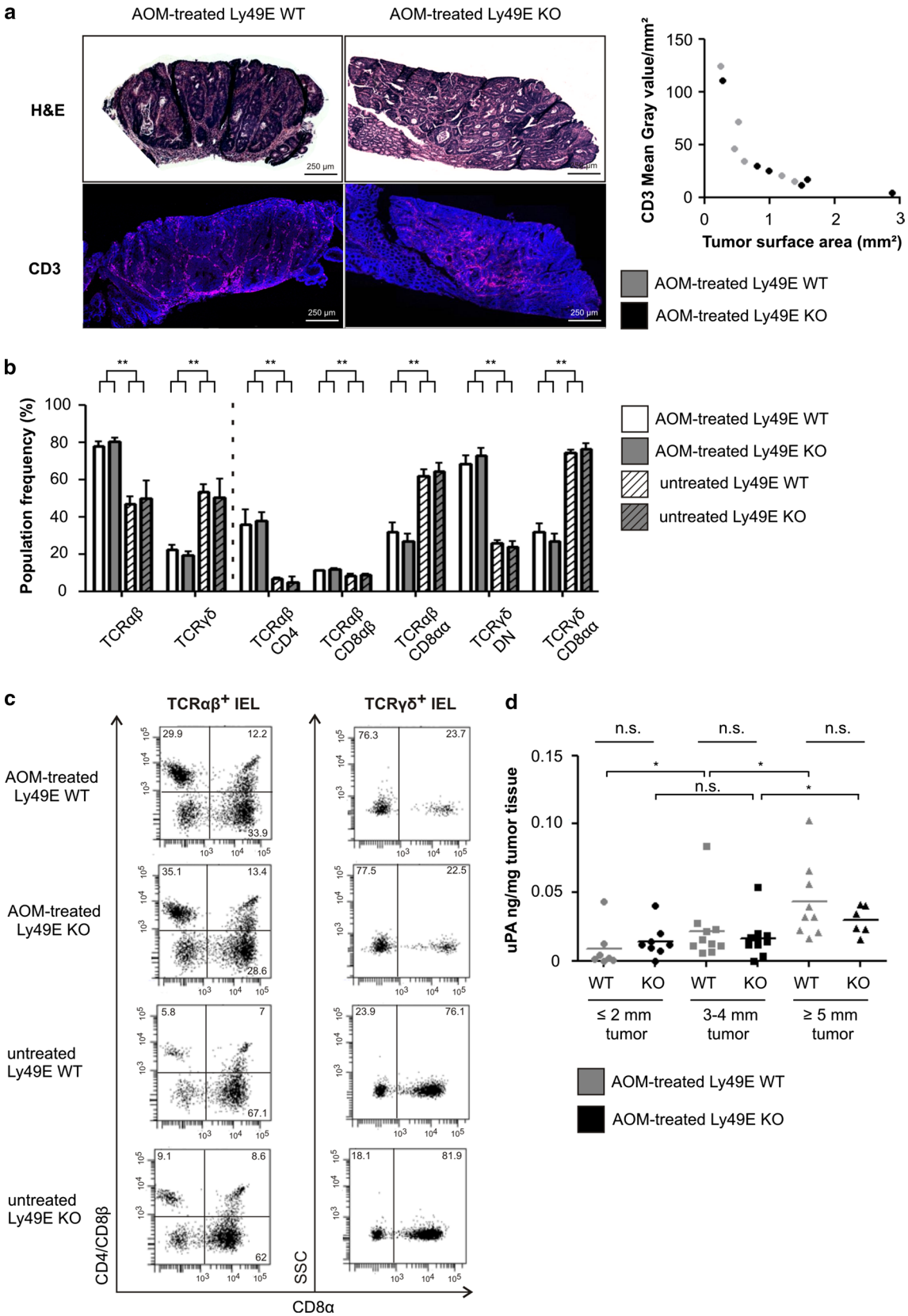
a
AOM-treated Ly49E WT
AOM-treated Ly49E KO
H&E
CD3
250 μm
CD3 Mean Gray value/mm²
Tumor surface area (mm²)
AOM-treated Ly49E WT
AOM-treated Ly49E KO
b
Population frequency (%)
TCRαβ
TCRγδ
TCRαβ CD4
TCRαβ CD8αβ
TCRαβ CD8αα
TCRγδ DN
TCRγδ CD8αα
AOM-treated Ly49E WT
AOM-treated Ly49E KO
untreated Ly49E WT
untreated Ly49E KO
c
TCRαβ+ IEL
TCRγδ+ IEL
AOM-treated Ly49E WT
AOM-treated Ly49E KO
untreated Ly49E WT
untreated Ly49E KO
CD4/CD8β
CD8α
SSC
d
uPA ng/mg tumor tissue
n.s.
WT
KO
≤ 2 mm tumor
3-4 mm tumor
≥ 5 mm tumor
AOM-treated Ly49E WT
AOM-treated Ly49E KO

◂**Fig. 4** Tumor-infiltrating T cells and tumor uPA expression in AOM-treated Ly49E WT versus Ly49E KO mice. **a** Hematoxylin/eosin-(H&E)- (*upper*), and CD3-(*lower*) stained paraffin tumor sections from AOM-treated Ly49E WT and Ly49E KO mice. *Scale bar* 250 μm, ×100 magnification. A graph showing CD3 mean gray value/mm^2 according to tumor surface area (mm^2) is shown for AOM-treated Ly49E WT and Ly49E KO mice ($n = 6$). **b** Colon tumor-infiltrating IEL subpopulation frequencies in AOM-treated Ly49E WT and Ly49E KO mice 14–22 weeks following the start of treatment, and colon IEL subpopulation frequencies from untreated Ly49E WT and Ly49E KO mice (mean ± SEM; $n = 5$ for AOM-treated mice; $n = 3$ for untreated mice). The percentage of TCRαβ and TCRγδ IEL is shown as a fraction of the total numbers of T cells. TCRαβ CD4, TCRαβ CD8αβ and TCRαβ CD8αα IEL subpopulation frequencies are shown as a percentage of the total TCRαβ IELs. TCRγδ DN and TCRγδ CD8αα IEL subpopulation frequencies are shown as a percentage of the total TCRγδ IEL. **c** Dot plots are shown for CD4/CD8β versus CD8α expression in colon tumor-infiltrating IEL in AOM-treated Ly49E WT and Ly49E KO mice, and colon IEL from untreated Ly49E WT and Ly49E KO mice. Numbers indicate the percentage of cells in each quadrant. Dot plots are representative for $n = 5$ AOM-treated mice and $n = 3$ untreated mice. **d** Tumor uPA expression in tumors of varying size from AOM-treated Ly49E WT and Ly49E KO mice at 14–22 weeks following the start of treatment. *n.s.* not significant. Data were analyzed using the nonparametric two-tailed Mann–Whitney *U*-test or the Kruskall–Wallis test. A p value ≤0.05, (*), a p value ≤0.01 (**) and p value ≤0.001 (***), were considered statistically significant

CD8αα-expressing IELs, and expression is higher for the colon as compared to the small intestine [14]. As such, we wished to explore a possible link between Ly49E and tumor immunosurveillance. It has been shown that the immune response not only protects against tumor development but can also select for tumor cells of lower immunogenicity [39]. If this also applies to the Apc$^{Min/+}$ model, tumors in Ly49E WT mice would be enriched for uPA production, whereas this would not be the case for tumors in Ly49E KO mice. However, our results show no significant difference in tumor uPA expression levels between Apc$^{Min/+}$ Ly49E WT and Apc$^{Min/+}$ Ly49E KO mice, indicating that interaction between Ly49E and uPA does not appear to influence the incidence or size of tumors arising in these mice.

Mice in the AOM-induced colorectal cancer model develop tumors along the aberrant crypt foci-adenoma-carcinoma sequence [29, 30]. This in contrast to Apc$^{Min/+}$ mice, where adenomas rarely progress to invasive adenocarcinoma's [28]. Thus, whereas Apc$^{Min/+}$ mice are excellent for study of the mucosa-adenoma transformation, study of AOM-treated mice may provide additional information with regard to adenoma-carcinoma transformation. To explore a possible role for Ly49E in later stages of colorectal cancer development, we treated Ly49E WT and Ly49E KO mice with AOM and monitored tumor development. Suzuki et al. [40] have previously shown that AOM-treatment does not influence body weight of mice. Similarly, we did not observe a difference in body weight between AOM-treated as compared to untreated mice, or between AOM-treated Ly49E KO and AOM-treated Ly49E WT mice. We observed no significant difference in colon length for AOM-treated Ly49E KO mice as compared to AOM-treated Ly49E WT mice. Following 14–22 weeks of AOM/DSS treatment, AOM-treated mice developed on average 5–10 tumors. Tumor distribution was similar for AOM-treated Ly49E KO mice as compared to AOM-treated Ly49E WT mice. Tumor load was comparable between AOM-treated Ly49E WT and Ly49E KO mice, and this for all time-points analyzed. Also, we did not observe a difference in numbers of tumors of any particular size.

Immunofluorescent staining of tumor sections from AOM-treated Ly49E WT and Ly49E KO mice showed that total T cell infiltration was comparable. Matsuda et al. [41] previously showed that the frequency of tumor-infiltrated TCRγδ cells is lower in well-to-moderately differentiated colorectal adenocarcinoma as compared to healthy colon IELs. Moreover, tumor-infiltrating lymphocytes were found to be predominantly CD4$^+$ and TCRαβ$^+$ [41]. Analyzing the frequencies of tumor-infiltrating lymphocytes in AOM-treated and untreated control mice, we similarly noted a significant decrease in the frequency of TCRγδ lymphocytes in colorectal tumors of AOM-treated mice. Alongside, we noted an increase in the frequency of TCRαβ lymphocytes, with a significant increase in the frequency of conventional TCRαβ CD4 and CD8αβ cells. In contrast, the frequency of CD8αα lymphocytes was significantly decreased in both the TCRαβ and TCRγδ cell fractions. However, no differences in infiltrating lymphocyte populations were observed between AOM-treated Ly49E WT and Ly49E KO mice, suggesting that Ly49E expression does not influence the total number or frequency of subpopulations of tumor-infiltrating lymphocytes.

uPA has been extensively implicated in the development of colorectal cancer development, where increased levels of both plasma and tissue uPA are present in patients with colorectal cancer [42]. Furthermore, increased uPA activity has been demonstrated for adenocarcinomas as compared with adenomatous polyps, showing that uPA expression levels correlate with colorectal cancer staging [43]. Examining uPA expression in tumors of varying size, we noted a gradual increase in relative tumor uPA expression as tumor size increased. There was a trend toward higher uPA expression in tumors from AOM-treated Ly49E WT as compared to Ly49E KO mice, but this was not significantly different. Thus, on the basis of these experiments, it would appear that Ly49E expression on intestinal IELs does not result in immunoediting of AOM-induced colorectal cancer cells.

In conclusion, we have shown that intestinal cancer, as modeled in Apc$^{Min/+}$ mice or through AOM/DSS treatment, is accompanied by significant changes in the gut. Specifically, study of tumor-infiltrating lymphocytes shows that

these cells are predominantly CD4 and CD8αβ TCRαβ cells. In contrast, the frequency of CD8αα-positive cells is reduced. Ly49E, expressed by IELs of the small intestine and colon, did not influence the frequencies of subpopulations of tumor-infiltrating lymphocytes in either model studied. Furthermore, Ly49E, triggered by uPA, did not influence relative tumor uPA expression levels. Thus, Ly49E expression on intraepithelial T lymphocytes does not affect the development or progression of intestinal cancer.

Acknowledgments We wish to thank Prof. Ria Cornelissen and Leen Pieters (Department of Basic Medical Sciences, Ghent University, Ghent, Belgium) for their aid in immunofluorescent staining of tumor sections.

Funding This work was supported by grants from the Foundation against Cancer, a foundation of public interest (2014-214) (G. Leclercq), by the Research Fund—Belgium (FWO) (G.0187.13N) (G. Leclercq), by the Interuniversity Attraction Pole (IUAP) grant T-Time from the Belspo Agency (Project P7/39) (B. Vandekerckhove, T. Taghon, G. Leclercq), and by the BOF of Ghent University (BOF11/GOA/005) (J. Plum, G. Leclercq, B. Vandekerckhove, T. Taghon). A. Van Acker and J. Filtjens are supported by the Institute for the Promotion of Innovation through Science and Technology Flanders (IWT-Vlaanderen). S. Taveirne and T. Kerre are supported by the FWO. D. Elewaut is supported by the Research Fund—Flanders (FWO) and the Research Council of Ghent University. D. Elewaut is also a member of a multidisciplinary research platform (MRP) of Ghent University and is supported by Interuniversity Attraction Pole (IUAP) grant Devrepair from the Belspo Agency (Project P7/07). E. Louagie is supported by Interuniversity Attraction Pole (IUAP) grant Devrepair from the Belspo Agency (Project P7/07).

Compliance with ethical standards

Conflict of interest The authors declare that they have no conflict of interest.

References

1. Bissahoyo A, Pearsall RS, Hanlon K, Amann V, Hicks D et al (2005) Azoxymethane is a genetic background-dependent colorectal tumor initiator and promoter in mice: effects of dose, route, and diet. Toxicol Sci 88:340–345
2. Haggar FA, Boushey RP (2009) Colorectal cancer epidemiology: incidence, mortality, survival, and risk factors. Clin Colon Rectal Surg 22:191–197
3. McClellan JL, Davis JM, Steiner JL, Day SD, Steck SE et al (2012) Intestinal inflammatory cytokine response in relation to tumorigenesis in the Apc(Min/+) mouse. Cytokine 57:113–119
4. Young PE, Womeldorph CM, Johnson EK, Maykel JA, Brucher B et al (2014) Early detection of colorectal cancer recurrence in patients undergoing surgery with curative intent: current status and challenges. J Cancer 5:262–271
5. Koido S, Ohkusa T, Homma S, Namiki Y, Takakura K et al (2013) Immunotherapy for colorectal cancer. World J Gastroenterol 19:8531–8542
6. Groh V, Steinle A, Bauer S, Spies T (1998) Recognition of stress-induced MHC molecules by intestinal epithelial gammadelta T cells. Science 279:1737–1740
7. Chen Y, Chou K, Fuchs E, Havran WL, Boismenu R (2002) Protection of the intestinal mucosa by intraepithelial gamma delta T cells. Proc Natl Acad Sci USA 99:14338–14343
8. Roberts AI, O'Connell SM, Biancone L, Brolin RE, Ebert EC (1993) Spontaneous cytotoxicity of intestinal intraepithelial lymphocytes: clues to the mechanism. Clin Exp Immunol 94:527–532
9. Ebert EC, Panja A, Praveen R (2009) Human intestinal intraepithelial lymphocytes and epithelial cells coinduce interleukin-8 production through the CD2–CD58 interaction. Am J Physiol Gastrointest Liver Physiol 296:G671–G677
10. Ebert EC, Groh V (2008) Dissection of spontaneous cytotoxicity by human intestinal intraepithelial lymphocytes: mIC on colon cancer triggers NKG2D-mediated lysis through Fas ligand. Immunology 124:33–41
11. Baker K, Foulkes WD, Jass JR (2009) MSI-H colorectal cancers preferentially retain and expand intraepithelial lymphocytes rather than peripherally derived CD8+ T cells. Cancer Immunol Immunother 58:135–144
12. Yokoyama WM, Plougastel BF (2003) Immune functions encoded by the natural killer gene complex. Nat Rev Immunol 3:304–316
13. Taveirne S, Filtjens J, Van Ammel E, De Colvenaer V, Kerre T et al (2011) Inhibitory receptors specific for MHC class I educate murine NK cells but not CD8alphaalpha intestinal intraepithelial T lymphocytes. Blood 118:339–347
14. Van Acker A, Filtjens J, Van Welden S, Taveirne S, Van Ammel E et al (2014) Ly49E expression on CD8alphaalpha-expressing intestinal intraepithelial lymphocytes plays no detectable role in the development and progression of experimentally induced inflammatory bowel diseases. PLoS One 9:e110015
15. Van Den Broeck T, Van Ammel E, Delforche M, Taveirne S, Kerre T et al (2013) Differential Ly49e expression pathways in resting versus TCR-activated intraepithelial gammadelta T cells. J Immunol 190:1982–1990
16. Van Den Broeck T, Stevenaert F, Taveirne S, Debacker V, Vangestel C et al (2008) Ly49E-dependent inhibition of natural killer cells by urokinase plasminogen activator. Blood 112:5046–5051
17. de Bruin PA, Griffioen G, Verspaget HW, Verheijen JH, Dooijewaard G et al (1988) Plasminogen activator profiles in neoplastic tissues of the human colon. Cancer Res 48:4520–4524
18. Duffy MJ (2005) Predictive markers in breast and other cancers: a review. Clin Chem 51:494–503
19. Protiva P, Sordat I, Chaubert P, Saraga E, Tran-Thang C et al (1998) Alterations in plasminogen activation correlate with epithelial cell dysplasia grading in colorectal adenomas. Br J Cancer 77:297–304
20. Sim PS, Stephens RW, Fayle DR, Doe WF (1988) Urokinase-type plasminogen activator in colorectal carcinomas and adenomatous polyps: quantitative expression of active and proenzyme. Int J Cancer 42:483–488
21. Sordat I, Chaubert P, Protiva P, Guillou L, Mazzucchelli L et al (1997) In situ stromal expression of the urokinase/plasmin system correlates with epithelial dysplasia in colorectal adenomas. Am J Pathol 150:283–295
22. Suzumiya J, Hasui Y, Kohga S, Sumiyoshi A, Hashida S et al (1988) Comparative study of plasminogen activator antigens in colonic carcinomas and adenomas. Int J Cancer 42:627–632
23. Ganesh S, Sier CF, Griffioen G, Vloedgraven HJ, de Boer A et al (1994) Prognostic relevance of plasminogen activators and their inhibitors in colorectal cancer. Cancer Res 54:4065–4071
24. Yang JL, Seetoo D, Wang Y, Ranson M, Berney CR et al (2000) Urokinase-type plasminogen activator and its receptor in colorectal cancer: independent prognostic factors of metastasis and cancer-specific survival and potential therapeutic targets. Int J Cancer 89:431–439

25. Dano K, Behrendt N, Hoyer-Hansen G, Johnsen M, Lund LR et al (2005) Plasminogen activation and cancer. Thromb Haemost 93:676–681
26. Killeen S, Hennessey A, El Hassan Y, Waldron B (2008) The urokinase plasminogen activator system in cancer: a putative therapeutic target? Drug News Perspect 21:107–116
27. Moser AR, Pitot HC, Dove WF (1990) A dominant mutation that predisposes to multiple intestinal neoplasia in the mouse. Science 247:322–324
28. Wang L, Zhang Q (2015) Application of the Apc(Min/+) mouse model for studying inflammation-associated intestinal tumor. Biomed Pharmacother 71:216–221
29. De Robertis M, Massi E, Poeta ML, Carotti S, Morini S et al (2011) The AOM/DSS murine model for the study of colon carcinogenesis: from pathways to diagnosis and therapy studies. J Carcinog 10:9
30. Neufert C, Becker C, Neurath MF (2007) An inducible mouse model of colon carcinogenesis for the analysis of sporadic and inflammation-driven tumor progression. Nat Protoc 2:1998–2004
31. Filtjens J, Taveirne S, Van Acker A, Van Ammel E, Vanhees M et al (2013) Abundant stage-dependent Ly49E expression by liver NK cells is not essential for their differentiation and function. J Leukoc Biol 93:699–711
32. Van Beneden K, De Creus A, Stevenaert F, Debacker V, Plum J et al (2002) Expression of inhibitory receptors Ly49E and CD94/NKG2 on fetal thymic and adult epidermal TCR V gamma 3 lymphocytes. J Immunol 168:3295–3302
33. Fraser KP, Gays F, Robinson JH, van Beneden K, Leclercq G et al (2002) NK cells developing in vitro from fetal mouse progenitors express at least one member of the Ly49 family that is acquired in a time-dependent and stochastic manner independently of CD94 and NKG2. Eur J Immunol 32:868–878
34. Hildenbrand R, Allgayer H, Marx A, Stroebel P (2010) Modulators of the urokinase-type plasminogen activation system for cancer. Expert Opin Investig Drugs 19:641–652
35. Puppa MJ, White JP, Sato S, Cairns M, Baynes JW et al (2011) Gut barrier dysfunction in the Apc(Min/+) mouse model of colon cancer cachexia. Biochim Biophys Acta 1812:1601–1606
36. McCart AE, Vickaryous NK, Silver A (2008) Apc mice: models, modifiers and mutants. Pathol Res Pract 204:479–490
37. Marsh L, Coletta PL, Hull MA, Selby PJ, Carding SR (2012) Altered intestinal epithelium-associated lymphocyte repertoires and function in ApcMin/+ mice. Int J Oncol 40:243–250
38. Ploplis VA, Tipton H, Menchen H, Castellino FJ (2007) A urokinase-type plasminogen activator deficiency diminishes the frequency of intestinal adenomas in ApcMin/+ mice. J Pathol 213:266–274
39. Dunn GP, Old LJ, Schreiber RD (2004) The three Es of cancer immunoediting. Annu Rev Immunol 22:329–360
40. Suzuki R, Kohno H, Sugie S, Tanaka T (2005) Dose-dependent promoting effect of dextran sodium sulfate on mouse colon carcinogenesis initiated with azoxymethane. Histol Histopathol 20:483–492
41. Matsuda S, Yamane T, Hamaji M (1998) CD4- and TCRalpha-beta-positive T lymphocytes predominantly infiltrated into well-moderately differentiated colon adenocarcinoma tissues. Jpn J Clin Oncol 28:97–103
42. Herszenyi L, Barabas L, Hritz I, Istvan G, Tulassay Z (2014) Impact of proteolytic enzymes in colorectal cancer development and progression. World J Gastroenterol 20:13246–13257
43. de Bruin PA, Griffioen G, Verspaget HW, Verheijen JH, Lamers CB (1987) Plasminogen activators and tumor development in the human colon: activity levels in normal mucosa, adenomatous polyps, and adenocarcinomas. Cancer Res 47:4654–4657